Acta Cryst. (1967). 22, 706

Structure of Ice V

By Barclay Kamb, Anand Prakash and Carolyn Knobler* California Institute of Technology†, Pasadena, California, U.S.A.

(Received 20 July 1966)

Ice V, the high-pressure ice phase stable at pressures of about 3 to 6 kbar, density 1.23 g.cm^{-3} , has a structure involving 28 H₂O molecules in a monoclinic cell of dimensions a=9.22, b=7.54, c=10.35 Å, $\beta=109.2^{\circ}$, space group A2/a. The structure is a single tetrahedral framework, rather than a 'self clathrate' as occurs in the denser forms ice VI and VII. Each oxygen atom is hydrogen bonded to 4 near neighbors at distances of 2.76-2.87 Å (average, 2.80 Å), and the shortest next-nearest neighbor distance is 3.28 Å. Distortion from ideal tetrahedral coordination is rather large, bond angles (at oxygen) ranging from 84 to 128° , with a r.m.s. deviation of 18° from 109.5° . There is no indication of bifurcated hydrogen bonds. Proton ordering is not possible in the space group A2/a indicated for the oxygen atoms. A proton-ordered structure is possible in space group Aa, but is considered unlikely on the basis of comparison with X-ray evidence for proton order in ice II. For the ice V structure to remain proton disordered on quenching to 120° K (the experimental conditions), the ordering energy must be less than $0.14 \text{ kcal.mole}^{-1}$.

Introduction

Among the several forms of ice, ice V occupies an intermediate position. Ices I, Ic, and III (of densities 0.92, 0.92, and 1.16 g.cm⁻³) have rather open, tetrahedrally linked structures that are analogs, topologically, of structures of SiO₂. In ice VI and ice VII (1.31 and 1.50 g.cm⁻³), on the other hand, relatively high densities are achieved by the 'self-clathrate' structural principle, in which two independent, tetrahedrally linked frameworks are incorporated into one another, each framework occupying void space in the other (Kamb & Davis, 1964; Kamb, 1965a). Since the density of ice V (1.23 g.cm⁻³) places it intermediate between the above groups of low and high-density forms, there is interest in ascertaining how the transition between the two structural principles is accomplished, and whether the silicate analogy continues to hold at transitional densities. The structure can be expected to add to an understanding of the energetics of hydrogen-bond bending and overlap for water molecules (Kamb, 1965b).

Preparation and identification of ice V

The ice samples studied were made by slowly cooling water at pressure 5 kilobars from 20°C to -20°C , then quenching in liquid nitrogen, and releasing to atmospheric pressure. Individual samples, held in 0.5 mm glass capillaries, were examined on the precession camera at a temperature of -175°C .

Powder photographs indicate spacings (Table 1) in general agreement with those reported for ice V by Bertie, Calvert & Whalley (1963). The metastable phase

* Present address: Chemistry Department, University of California, Los Angeles, California, U.S.A.

ice IV, which is reported to occur within the stability field of ice V, might be expected to form initially in preference to V (Bridgman, 1935, p. 602). In extensive experiments in the stability region of ice V, we have obtained no second phase, and we have consistently obtained the phase identified in Table 1, from ices II and VI as well as from the liquid. In the course of making dielectric measurements on ice under pressure, Wilson, Chan, Davidson & Whalley (1965, p. 2385) located phase boundaries that agree better with the phase boundaries for ice V, as determined originally by Bridgman (1912), than with those for ice IV (Bridgman, 1935). It is not certain that this identification is applicable to the powder pattern designated as that of ice V by Bertie et al. (1963), because the latter was obtained from samples made in different apparatus and quenched to 77°K. However, in X-ray study of ice under pressure (Kamb & Davis, 1964), the same powder pattern is found at pressures of about 5 kbar (Table 1), and no other pattern, attributable to ice IV, has so far been obtained near this pressure.

The densities of ice V, VI, and VII, as determined from the X-ray powder patterns under pressure (Table 1; Kamb & Davis, 1964, Table 2), are listed in Table 2. For ice VII the determination is direct, while for ice V and VI it is based on the calculated densities of the quenched crystals, scaled in accordance with the average shift $\Delta d/d$ of the observed line spacings d in the high-pressure powder patterns relative to the calculated spacings for the quenched crystals. In the next to last line of Table 2, the X-ray densities are corrected to higher temperature, where they can be compared with densities measured volumetrically by Bridgman (1912, 1942). The expansion correction is made with an assumed volumetric thermal expansion of $1.1 \times$ 10⁻⁴°C⁻¹, which is thought to be reasonable (Kamb, 1965b). For ice VII and ice VI, our densities are systematically high relative to Bridgman's. The cause of

[†] Division of the Geological Sciences, Contribution No. 1401.

this discrepancy is not known. However, from the comparison in Table 2, the X-ray density of ice V as determined here (Table 2) is evidently compatible with Bridgman's density for ice V and not with his density for ice IV. This reinforces the identification of the form of ice studied here as ice V.

X-ray data

The unit cell of ice V, determined from precession photographs with Cu $K\alpha$ radiation of assumed wavelength 1.542 Å, is monoclinic with dimensions $a = 9.22 \pm 0.02$, $b = 7.54 \pm 0.01$, $c = 10.35 \pm 0.02$ Å, $\beta = 109.2 \pm 0.2^{\circ}$. Extinctions occur for reflections hkl with k+l

odd, and h0I with h odd. The space group is either A2/a or Aa. This cell accounts for the observed powder pattern (Table 1).

Intensity measurements were obtained from precession photographs of two single crystals, using Zr-filtered Mo $K\alpha$ radiation. Seventeen reciprocal lattice planes were photographed, involving 6 different orientations of the precession axis. Because of variation in image shape within and between films, which tends to occur for sample capillaries tilted away from the spindle axis and toward the precession axis, variable 'external' weights varying from 1.0 to 0.1 were assigned to the individual intensity readings. Readings for different films or film-groups were corrected for Lorentz and

Table	1.	X-ray	powder	data	for	ice	V
45		/45	(0)	•	(0)		

			-	-	uiu joi ice			
Notes (5)		(4)	(1)	(2)	(3)	(1)	(2)	(3)
F_o^2	hkl	d_{calc}	P = 0	P = 0	P = 5kb	I_1	I_2	I_3
3 3	200	3.37			3.28			5
3	211	3.23			3.18			10
42	122	3.03	3.03	3.02	2.96	S	80	50
58	013	2.99						
86	213	2.91	2.93	_	2.85	S	_	90
50	220	2.85						
40	220	2.85	2.86	2.82	2.80	S	100	100
96	311	2.85						
12 12	202 222	2.83	2.75					
	122	2.73	2.75	2 65	2 (2	w	100	100
130 37	122 204	2·67 2·52	2.68	2.65	2.63	S	100	100
. 12	313	2·32 2·49	2.52		2·52 2·47	mw		10
. 12 49	004	2.49	2.45	2.43	2·47 2·41		30	20
25	T31	2.40	2.43	2.43	2.41	m m	30	10 25
18	320	2.30	2.40	_	2.37	m	_	23
16	320	2.30	2.29	2.29	2.26	m	20	20
71	402	2.29	2 2)	2 2)	2 20	""	20	20
16	400	2.18		2.19	2.16		8	5
21	231	2.06	2.05	2.05	2.00*	m v	20	15
26	024	2.05			_ **	•••		
14	331	1.95		1.96	1.93		30	15
61	324	1.95						
40	411	1.92	_		1.90			10
25	040	1.89						
62	204	1.88		1.88	1.86		30	15
25	315	1.88						
41	<u>1</u> 42	1.77		1.78	1.74†		15	50
44	2 06	1.72		1.72	1.70		15	20
34	433 433	1.64		1.63			8	
18	Ī26	1.55		1.56			10	
19	602	1.54		1 40				
18	044	1.49		1.49			8	
11 12	გექ 135	1·48 1·46						
12 14	600	1·46 1·45		1.44			10	
13	342	1.43		1.44			10	
15	342 126	1.43		1.38			10	
14	615	1.38		1.30			10	
14	013	1.30						

⁽¹⁾ Spacings measured in powder patterns of present work. Intensities I estimated qualitatively. s=strong, m=medium, mw=medium-weak, w=weak.

(2) Spacings and intensities of quenched ice V reported by Bertie, Calvert & Whalley (1963).

(4) Spacings calculated from cell constants given in text.

* Overlapped by Be line.

⁽³⁾ Spacings and intensities for ice V at pressure 5 kbar, temperature -50° C, obtained by method of Kamb & Davis (1964). Diamond internal standard used for calibration, with assumed compressibility 0.18×10^{-6} bar⁻¹.

⁽⁵⁾ Square of observed structure factor from single-crystal measurement, divided by scaling factor of 100. Reflections having structure factor F_0 less than 33 omitted, except for first two entries in table.

[†] Overlapped by Be and diamond lines.

polarization factors and were scaled together by least-squares fit to the common reflections. No absorption correction was applied. The discrepancies of scaled individual intensity readings from the averages for common reflections are approximately 11% of the intensity values. The data list includes all reflections out to $\sin \theta/\lambda = 0.5 \text{ Å}^{-1}$, plus an incomplete sampling out to 0.72 Å^{-1} . Of the 913 reflections listed, measurable intensities were detected for 472, and for the remainder a limit of detection is known.

Structure determination

From the relative cell volumes of quenched ice V and VI, from the relative densities as measured by Bridgman (1912), and from the cell content of ice VI (Kamb, 1965a), the cell content of ice V is indicated to be 28 water molecules, for which the calculated density at 1 atm and -175 °C is $1\cdot231$ g.cm⁻³ (Table 2).

A statistical test of the X-ray intensity data (Howells, Phillips & Rogers, 1950) indicates centrosymmetry, hence space group A2/a. Because the general position in this space group has eightfold multiplicity, there must be at least 4 molecules in fourfold special positions, and there could be 12. Four of the five fourfold special positions in the space group, 4(a-d), are at centers of symmetry and are thus unsuited for a water molecule in roughly tetrahedral coordination. The remaining special position, 4(e), is on the twofold axis. With 12 molecules in 4(e), the average distance between them, along the twofold axis, would be 2.51 Å, too short for a hydrogen bond in ice. Hence only one position of type 4(e) must be occupied, and the remaining 24 molecules must occupy three general positions 8(f).

In the Patterson function for ice V, the expected tetrahedral grouping around the molecule in 4(e) is recognizable in terms of pairs of vector peaks of type (u, v, w), (2u, 2v, 0) where (u, v, w) is 2.8 Å from the origin and $w \simeq \frac{1}{4}$. Two pairs of this type, although not well resolved from other vectors, give an indication of the configuration of the tetrahedral group around position

4(e), and imply rough x and z coordinates $(x=\frac{1}{4}+u, z=w)$ for two of the oxygen atoms in 8(f). There is also a vector peak of type (u,v,0) $2\cdot 8$ Å from the origin, which suggests that the fourth molecule in 8(f) is so placed as to bond to its symmetry-equivalent molecule across the twofold axis. This fixes its x and z coordinates. With x and z coordinates determined for all the oxygen atoms, a reasonable scheme of tetrahedral coordination can be constructed, and rough y coordinates can be derived from the considerations that the bond lengths should be about $2\cdot 8$ Å and that no nonbonded oxygen-oxygen distance should be less than about $3\cdot 2$ Å.

Refinement

The structure so derived gave initially a structurefactor residual R of 52%. Refinement by electron density projections on (100), (010), and (001) reduced R to 28%, and least-squares refinement with allowance for anisotropic thermal motion of oxygen atoms further reduced R to 12%. (Scattering factors used are those of Hoerni & Ibers (1954) for oxygen, and of International Tables for X-ray Crystallography (1962) for hydrogen). A difference map, discussed in a later section, suggested that hydrogen, hitherto omitted from the calculation, should be introduced in the form of 4 atoms with population factor $\frac{1}{2}$ in roughly tetrahedral orientation around each oxygen atom. Since the intensity data are inadequate to justify a refinement of hydrogen coordinates, hydrogen atoms with population factor \(\frac{1}{2} \) were placed arbitrarily in positions along the lines of centers between pairs of oxygen atoms and 1.0 Å from each end. The final refinement, results of which are listed in Table 3, gave a residual R= $\Sigma |F_o - F_c|/\Sigma |F_o|$ of 9.9%, and a weighted residual $\sum w(F_o^2 - F_c^2)^2/\sum wF_o^4$ of 4.0%. The weights w used in least-squares refinement were taken proportional to the external weights assigned earlier (combined in accordance with the number of independent intensity observations) and to $(1 + \sin^2\theta/\sin^2\theta_{\text{max}})^2 \cdot (F_o^2 + 15^2)^{-2}$, where θ_{max} is the largest observed Bragg angle of

Table 2. Densities of ice phases(a)

Ice phase	VII	VI	V	IV
g_c at 1 atm, -175° C (g.cm ⁻³)	$1.50^{(b)}$	1.314	1.231	
$\langle \Delta d/d \rangle$ at P, T_1		0.016	0.014	
ϱ_c at \dot{P} , T_1 (g.cm ⁻³)	1.66	1.377	1.283	
$P(kbar)^{(c)}$	25	8.0	5.3	5∙4
$T_1(^{\circ}C)$	-50	50	 50	
T_2 (°C)	+25	+15	- 5	-6
ϱ_0 at P , T_2 (g.cm ⁻³)	1.565	1.345	1.260	$1.29^{(d)}$
ϱ_c corrected ^(e) to P , T_2	1.65	1.367	1.277	
Uncertainty (f) in corrected ϱ_c	±0.016	± 0.013	± 0.013	

⁽a) Calculated densities ϱ_o based on X-ray spacings and cell contents. Measured densities ϱ_o from volumetric measurements by Bridgman (1912, 1935, 1942).

(b) From powder data of Bertie, Calvert & Whalley (1963).

(e) Expansion correction based on assumed thermal expansion of $1 \cdot 1 \times 10^{-4} \, ^{\circ}\text{C}^{-1}$.

⁽c) Sample pressure in X-ray measurements is uncertain because of piston friction and is known to about ± 2 kbar only. (d) Density determined indirectly from measurements by Bridgman (1935) on D_2O ice, by assuming that the molar volume difference between ice IV and ice VI is the same for D_2O and H_2O ices.

⁽¹⁾ Uncertainty based on scatter in the $\Delta d/d$ values for the stronger peaks ($I_3 > 10$), plus possible 50% error in the thermal expansion correction.

Table 3. Observed and calculated structure factors

L designates unobserved reflections, for which the limit of detection is listed under F_o . * designates reflections assigned zero weight because they were detected on some films at a level higher than the detection on other films where they were not detected.

### ### #### #########################	-9 1 1 7 8 -17 -7 7 7 7 4 L L 1 7 7 7 7 7 7 L L 1 1 7 7 7 7 7 4 L L 1 1 7 7 7 7 7 7 L L 1 1 1 1 2 2 1 1 1 1 1 2 2 2 2 2 2 L L 1 1 1 1	-5 + 4 + 4 + 1 13 12 12 13 12 13 13	-2 0 0 6 8 8 5 19 18 17 7 12 20 0 6 8 18 5 19 17 7 12 20 12	0 6 18 * 11 14 0 6 10 L 8 2 0 7 1 22 - 22 0 7 5 * 12 - 12 0 7 7 5 * 12 - 12 0 7 7 9 L 8 - 2 0 8 2 * 6 - 4 0 8 6 7 5 0 8 8 L 7 5 0 8 8 L 7 5 0 9 1 L 8 - 5	-24 B 8 4 6 1 1 1 1 1 2 2 9 6 3 6 6 6 6 7 7 7 8 8 8 9 9 9 1 1 1 1 2 2 2 2 2 2 2 2 2 2 2 2 2	Po 87448711469400641205258811626175791212171717192142458162027114411817211521721152171719277143630420137716410 Po 87448714114111812171171908141181171719217171717171717171717171717171717	P. 117.6 1.1 1
--	---	---	---	---	---	--	--

about 30°, and 15 represents a structure factor about 50% greater than the general limit of observation. The dependence on θ is introduced to give greater weight to the higher-order reflections. Zero weight (marked (*) in Table 3) was assigned to reflections which were detected on some films at a level higher than the observational limit for other films on which they were not detected; in general these reflections are close to the limit of detection. Final least-squares parameter shifts were less than 0.0002. The refined parameters are listed in Table 4.

Description of the structure

The structure of ice V is shown in Fig. 1, as viewed along the b axis. It consists of a tetrahedral framework in which each oxygen atom is surrounded by four others at distances of about 2.8 Å, typical of hydrogenbond distances in other forms of ice. The structure can be visualized as built up of zigzag chains of water molecules running parallel to the a axis of the crystal. One type of chain consists alternately of O(2) and O(3) atoms, while a second type consists wholly of O(4) atoms (Fig. 1). These chains resemble zigzag chains that occur linked together in the puckered hexagonal sheets parallel to (0001) in ice I, hence the rough similarity in the axial lengths 2a=9.00 in ice I and a=9.22 Å in ice V. O(2)-O(3) chains bond in pairs to O(4)-O(4) chains in such a way as to build up tetrahedrally linked layers parallel to (001) (these layers are quite different from the layers parallel to (0001) in ice I). There are two such layers in the ice V cell, centered about z=0and $z=\frac{1}{2}$. Linkage between O(2)-O(3) chains in the layers is completed by the O(1) atoms, which lie at the centers of the layers. Adjacent layers are then linked together by the bonds from O(1) of one layer to O(3)of adjacent layers (Fig. 1), resulting in a three-dimensional tetrahedral framework.

Coordination distances and angles for the oxygen atoms in ice V are given in Table 5. The shortest distances, listed as hydrogen-bond distances in Table 5, are all less than 2.9 Å, and, with exception of the long O(4)-O(4') distance of 2.867 Å, fall in the range 2.76-2.82 Å. The two shortest distances that are longer than these, for each oxygen atom, are listed in the Table as non-bonded. The short non-bonded distances of

3.28 and 3.46 Å are labeled in Fig. 1. Distances in Table 5 have estimated standard deviations in the range 0.004 to 0.006 Å, angles from 0.2° to 0.3°. The coordination angles (Table 5) indicate a considerable deviation from ideal tetrahedral coordination around the water molecules.

Hydrogen bonding

When the coordination around water molecules becomes increasingly distorted from the ideal tetrahedral one, as it does in the denser forms of ice, the possibility arises that some of the oxygen-oxygen distances near 2.8 Å are not hydrogen bonds but simply van der Waals contacts, appropriate to van der Waals radius 1.40 Å for oxygen (Pauling, 1960, p. 260). Non-hydrogen-bonded intermolecular oxygen-oxygen contacts of 2.7 to 2.9 Å have been found in organic molecular crystals (Prakash, 1965; Craven & Takei, 1964) and in crystalline H₂O₂ (Abrahams, Collin & Lipscomb, 1951). There

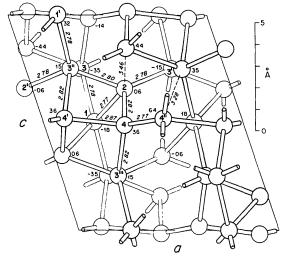


Fig. 1. Structure of ice V, as viewed along the b axis. Only the oxygen atoms are shown. Hydrogen bonds between water molecules are represented by rods, with oxygen-oxygen distances as labelled, the hydrogen atoms being omitted. Unit cell outlined spans the area $0 \le x \le 1, -\frac{1}{2} \le z \le \frac{1}{2}$ in relation to coordinates listed in Table 4. y coordinates of oxygen atoms are given in hundredths of the b axial length (7.54 Å), y increasing upward out of plane of projection (axial system as arbitrarily plotted is left-handed). Two short non-bonded distances are indicated by dashed lines. Oxygen atoms are labelled to correspond with Tables 4 and 5.

Table 4. Oxygen coordinates and thermal parameters in ice V Estimated standard deviations (in last decimal place) noted in parentheses. Temperature factor in form exp $(-\beta_{11}h^2 - \beta_{22}k^2 - \beta_{33}l^2 - \beta_{12}hk - \beta_{23}kl - \beta_{31}lh)$.

		Position	x	y	z	
	O(1)	4(<i>e</i>)	0.2500	-0.1847(8)	0.0000	
	O(2)	8(f)	0.4629 (4)	0.0565 (5)	0.1544 (4)	
	O(3)	8(f)	0.2751 (4)	-0.3475(6)	0.2477 (4)	
	O(4)	8(<i>f</i>)	0.3993 (4)	0.3596 (5)	-0.0146(4)	
	β_{11}	β_{22}	β_{33}	β_{12}	β_{23}	β_{31}
O (1)	0.0092	0.0119	0.0040	0.0000	0.0052	0.0000
O(2)	0.0072	0.0080	0.0067	0.0007	0.0052	-0.0008
O(3)	0.0083	0.0081	0.0053	-0.0007	0.0048	0.0004
O(4)	0.0084	0.0077	0.0060	-0.0012	0.0049	0.0005

is the further possibility of bifurcated hydrogen bonds. A bifurcated bond involving intermolecular oxygen-oxygen distances of 2.79 and 2.96 Å is known (Craven & Takei, 1964), and bifurcated bonds of distances 2.47 to 2.87 Å are surmised (Craven, Martinez-Carrera & Jeffrey, 1964).

However, such structural features do not occur in ice V. Identification of the oxygen-oxygen distances less than 2.9 Å as simple hydrogen bonds follows from the fact that there are just four such distances for each water molecule and that these distances, which cluster closely around 2.80 Å, are well distinguished from the longer distances of 3.28, 3.45, ... A. A similar situation holds in ice I, Ic, II, III, and VI, where the range of hydrogen bond lengths is 2.75 to 2.84 Å (Peterson & Levy, 1957); Honjo & Shimaoka, 1957; Kamb & Datta, 1960; Kamb, 1964, 1965a). In spite of the considerable angular distortion from ideal tetrahedral coordination in ice V (Table 5), there are no O···H₂O ··· O coordination angles approaching 60°, which is considered by Craven, Martinez-Carrera & Jeffrey (1964, p. 901) to be the upper limit for acceptance of a bifurcated hydrogen bond, and there is no increase in number of near neighbors over 4, as could be expected if bifurcated bonds were formed. A tetrahedral framework of bent hydrogen bonds is indicated.

This conclusion is consistent with the infrared and Raman spectra of ice V, the OH stretching frequencies being increased by only about 70 cm⁻¹ relative to ice I, as compared with an increase of 400 cm⁻¹ for water vapor (Bertie & Whalley, 1964).

Although the O(4)-O(4') distance of 2.867 Å is conspicuously long (the longest nearest-neighbor distance

in any form of ice except ice VII), there is no indication that it is non-bonded. The tetrahedral coordination around O(4) is no more distorted than that around other oxygen atoms in the ice V structure. A significant amount of bifurcation toward the close next-nearest neighbor O(3*) at 3.28 Å is unlikely, because of the disparity in distances, the unfavorable orientation of O(3*) relative to nearest neighbors O(2) and O(4''), and the O(4') \cdots O(4) \cdots O(3*) angle of 80°. The O(4) O(4') distance is 0.06 Å shorter than the non-bonded O···O contact in hydrogen peroxide, whereas a non-bonded contact for H₂O should be longer.

The van der Waals radius of 1.40 Å for oxygen. while appropriate to oxygen-oxygen contacts in larger molecules, does not describe the non-hydrogen-bonded equilibrium distance between water molecules. The evidence from ice VII (Kamb, 1965a) indicates that a rather strong repulsion operates between non-hydrogen-bonded water molecules at a distance of 2.95 Å, and suggests that the equilibrium separation should be about 3.5 Å. The ice VI structure (Kamb, 1965a) indicates a weak repulsion between non-bonded water molecules at 3.51 Å. In crystals of diatomic gases involving C, N, O, and F, the following shortest nonbonded interatomic distances (interatomic van der Waals contacts) occur: α -N₂, 3.42 Å; γ -O₂, 3.41 ņ; β-F₂, 3·33 ņ; CO, 3·58 Å (Jordan, Smith, Streib & Lipscomb, 1964; Jordan, Streib, Smith & Lipscomb, 1964; Jordan, Streib & Lipscomb, 1964; Barrett & Meyer, 1965; Vegard, 1930). Other things being equal,

 \dagger Between molecules centered at positions 6(k), for which the known type of rotational disorder allows the intermolecular distance to be interpreted as a minimum interatomic distance.

Table 5. Coordination data for oxygen atoms* in ice V

Hydrogen bond distances ($\sigma \le 0.006 \text{ Å}$)								
O(1)-O(2) O(1)-O(3) O(2)-O(3')	2·766 Å 2·782 2·781	O(4)-O(4") O(4)-O(3)"' O(4)-O(2)	2·766 Å 2·819 2·820					
O(2)-O(3'')	2.798	O(4)-O(4')	2.867					
Shortest non-bonded distances								
O(3)-O(4*)	3.277	O(2')-O(3'')	3.493					
O(1)–O(4*) O(2)–O(2*)	3·449 3·465	O(1) - O(2*)	3.644					
Bond angles at oxyger	` = '							
O(2)-O(1)-O(3)	86·0°†	O(1)—O(2)–O(3")	83·5°					
O(2)-O(1)-O(2")	97·8	O(1)— $O(2)$ — $O(3')$	101.8†					
O(3)-O(1)-O(3*)	127.6	O(1)—O(2)—O(4)	102.2					
O(3)-O(1)-O(2'')	130.6	O(3') - O(2) - O(3)''	134.9					
		O(3') - O(2) - O(4)	131.6					
		O(3'')-O(2)-O(4)	89·3†					
O(1')-O(3'')-O(2)	127.6	O(2)O(4)-O(3"')	92.0†					
O(1')-O(3'')-O(2')	112.6	O(2)O(4) - O(4')	86.9					
O(1')-O(3'')-O(4')	116·5†	O(2) - O(4) - O(4'')	123.9					
O(2) - O(3'') - O(2')	114·3†	O(3''')-O(4)-O(4')	87.9					
O(2) -O(3'') -O(4')	88.2	O(3''')-O(4)-O(4'')	125.8					
O(2')-O(3'')-O(4')	86·6	O(4')—O(4)–O(4'')	128.5†					

^{*} Oxygen atoms are labelled to conform to Fig. 1. Atoms identified with an asterisk are not labelled in Fig. 1.

[†] Donor angles in a possible ordered proton arrangement in Aa that utilizes angles as near as possible to 109.5° and gives a half-hydrogen model as seen in space group A2/a.

these distances should be somewhat shorter than the equilibrium van der Waals contact between non-hydrogen-bonded water molecules, because the dispersion forces between the diatomic molecules are somewhat larger as suggested by their molar refractions and by virial coefficient data (Hirschfelder, Curtiss & Bird, 1964, pp. 165, 1034, 1112)‡. For CO₂ the attractive forces are several times larger, and the $O \cdots O$ contacts shorten to 3.20 Å (Krüner, 1926). A comparable shortening should occur in comparing the van der Waals distances for H₂O and hydrogen peroxide. Under the effect of hydrogen bonds strongly stretched to 2.95 Å. the van der Waals contact between H₂O molecules in ice VII (equal number of stretched hydrogen-bonds and compressed van der Waals contacts) shortens to 2.95 Å, while under hydrogen-bonds stretched to only 2.80 Å in crystalline hydrogen peroxide (again equal numbers of bonds and contacts), the O···O contact distance is only slightly shorter, 2.93 Å (from parameters by Busing & Levy, 1965).

Proton disorder

An important feature of ice structures is the degree of disorder of the proton positions. For ice V, a proton-ordered structure is not possible in space group A2/a, because oxygen atoms of type O(4) bond to one another across twofold axes and symmetry centers, a situation not compatible with the asymmetry of the hydrogen bonds as required by the bond lengths (Table 5).

This conclusion is supported by an $(F_o - F_c)$ synthesis calculated from the X-ray data after refinement of oxygen positions and anisotropic thermal motions but before inclusion of hydrogen atoms. In this difference map there are 16 peaks, of height 0.2 to 0.6 e.Å-3, listed in Table 6. For comparison are listed coordinates of the 14 non-equivalent points lying on centerlines between hydrogen-bonded oxygen atoms and 1.0 Å from each oxygen position. Thirteen of these possible proton sites match roughly with peaks in the difference map. The estimated standard deviation of the electron density (Rollett, 1965, p. 108) is 0·14 e.Å-3, which agrees with the common occurrence of values +0.1 e.Å-3 in the map at points distant from oxygen or possible hydrogen positions. This noise level is sufficient to account for the fluctuations in heights and discrepancies in position of peaks attributable to hydrogen at the 14 possible sites, and to account for the three unattributable peaks.

The average electron density at the centerline proton sites (Table 6) is 0.3 e.Å^{-3} , one-half the density 0.6 e.Å^{-3} commonly found for hydrogen in structures for which the refined residual R is about 10%. After introducing half-hydrogen atoms at these sites, with isotropic temperature parameter $B = 2.0 \text{ Å}^2$, the average difference density at the sites is reduced to zero. Hence in space group A2/a, a proton-disordered structure for ice V is indicated, having protons at all of the 14 possible sites, with occupancy probability $\frac{1}{2}$. It corresponds to the type of proton arrangement in ice I (Pauling, 1935; Peterson & Levy, 1957). (There is no special merit to 'average' proton positions lying exactly on the oxygen-oxygen center lines, as chosen in Table 6, but

Table 6. Data for hydrogen positions

			14010 0. 24	jo	Transfer Land			
								on density
			Coord	dinates			At	At calculated
	Fr	om $(F_o - F_c)$ n	nap	Calcul	lated on cent	er lines	peak	position
Atom*	x	У	z	x	y	z	$(e.A^{-3})$	$(e.Å^{-3})$
$H_1(1)$	0.33	-0.13	0.06	0.33	 0·10	0.06	0.5	0.4
$H_1(2)$	0.26	-0.26	0.08	0.26	 0·24	0.09	0.4	0.4
$H_2(1)$	0.41	-0.03	0.10	0.39	-0.03	0.10	0.5	0.3
$H_2(2)$	_			0.38	0.09	0.19	0.0	0.0
$H_2(3)$	0.44	0.15	0.11	0.44	0.17	0.09	0.4	0.3
$H_2(4)$	0.55	-0.02	0.19	0.56	-0.02	0.19	0.6	0.5
$H_3(1)$	0.25	-0.27	0.17	0.27	-0.29	0.16	0.3	0.3
$H_3(2)$	0.36	-0.40	0.29	0.37	-0.42	0.28	0.3	0.3
$H_3(3)$	0.32	-0.25	0.32	0.32	-0.27	0.33	0.4	0.3
$H_3(4)$	0.17	-0.38	0.27	0.19	-0.38	0.28	0.2	0.2
$H_4(1)$	0.43	0.26	0.04	0.42	0.25	0.05	0.4	0.3
$H_4(2)$	0.29	0.35	-0.04	0.29	0.36	0.00	0.5	0.2
$H_4(3)$	0.33	0.29	-0.08	0.36	0.29	-0.10	0.3	0.2
$H_4(4)$	0.45	0.47	0.01	0.47	0.46	0.00	0.4	0.4
+	0.57	0.04	0.18				0.6	
+	0.35	0.04	0.11				0.5	
'	0.19	0.32	0.06				0.4	

^{*} Subscript indicates oxygen atom to which the hydrogen atom is covalently bonded.

† Peaks not correlated with a calculated hydrogen position.

[‡] However, the virial coefficient interpretations for H_2O yield an anomalously low repulsive potential between water molecules and hence predict a short equilibrium van der Waals distance of 3.06 Å. This appears to arise from approximations in the treatment of the hydrogen-bond interaction (Kamb, 1965b, p. 3922).

[§] The fictitiously low value of B needed is in accord with experience for other structures (Jensen & Sundaralingam, 1964).

experimental errors prevent a reliable determination of the proton positions from the X-ray data).

A possibility remains that long-range proton ordering could take place in a space group of lower symmetry, and that the observed space group A2/a could represent only an approximate symmetry defined by the framework of oxygen atoms. This situation occurs in ice II (Kamb, 1964), where the oxygen atoms define a framework with pseudo-cell in $R\overline{3}c$, whereas the actual cell is degraded to R3 by small displacements of the oxygen atoms in response to proton ordering at the lower symmetry. If the oxygen displacements upon proton ordering in ice V would be comparable to those that occur in ice II, then triclinic space groups can be ruled out by the lack of detectable violation of the a-glide extinction. Likewise A2, and monoclinic space groups without the A centering, are ruled out. and the sole possibility is Aa.

Ordered proton arrangements can be formulated for ice V in space group Aa, based on the oxygen framework in A2/a. The question arises whether the anisotropy of the apparent thermal motions (Table 7) could reflect small displacements of the oxygen atoms in accordance with symmetry Aa, away from average positions in A2/a. Such a situation is similar to what would be encountered in ice II if the reflections hhl with l odd were ignored, so that the symmetry-degrading displacement perturbations would have to be recognized from their effects on intensities of reflections common to the true cell and the pseudo-cell. To allow comparison between these two cases, we have refined the ice V structure isotropically in Aa and the ice II structure anisotropically in $R\bar{3}c$. The apparent thermal motion anisotropy in the $R\bar{3}c$ structure for ice II is only slightly larger than that in the A2/a structure for ice V (Table 7). However, for ice II the structure factor residual R (omitting hhl with l odd) drops from 14.4%for the anisotropic $R\overline{3}c$ structure to 7.9% for the isotropic $R\overline{3}$ structure, whereas for ice V it rises slightly from 9.9% for A2/a (anisotropic) to 10.2% for Aa(isotropic). There is thus no indication of an ordered structure for ice V in Aa.

Table 7. Apparent thermal-motion ellipsoids

Structure	Atom	Principal axes B_i
Ice V, A2/a	1	$(Å^2)$ 2.81, 2.71, 1.41
ice v, A2/u	2	2.57, 2.17, 1.74
	3	2.52, 2.01, 1.78
	4	2.58, 2.28, 1.72
Ice II, $R\overline{3}c$	1	3.18, 1.76, 1.18

Infrared spectrum

The lack of resolved fine structure in the $\nu_{\rm OD}({\rm HDO})$ and $\nu_{\rm OH}({\rm HDO})$ bands of quenched ice V, and the rather large half-widths of these bands, can be interpreted alternatively as due either to a disordered proton arrangement in a small unit cell or to an ordered

arrangement in a large cell (Bertie & Whalley, 1964, p. 1657). The bands of ice II (Bertie & Whalley, 1964), in contrast, are resolved into sharp lines, and the number of lines (four for $\nu_{\rm OD}$, three for $\nu_{\rm OH}$ with one close pair unresolved) correlates with the four non-equivalent hydrogen bonds present in the proton-ordered ice II structure (Kamb, 1964). In a possible proton-ordered structure for quenced ice V (in space group Aa), 14 non-equivalent bonds would contribute absorption lines spanning the observed band widths $150\,\mathrm{cm^{-1}}$ (for $\nu_{\rm OH}$) or $80\,\mathrm{cm^{-1}}$ ($\nu_{\rm OD}$). If equally spaced, the lines would have separations of about $10\,\mathrm{cm^{-1}}$ or $5\,\mathrm{cm^{-1}}$, and if unequally spaced, which is probable, there would be clusters of lines with greater separations between them.

The resolutions actually achieved for ice II and III are about 12 cm^{-1} (ν_{OH}) and 8 cm^{-1} (ν_{OD}), and there is no evident structural reason why the intrinsic line widths should be much greater for ice V than for ice II and III. Hence a proton-ordered ice V (in Aa) would necessarily show appreciable resolution and fine structure in the $\nu_{OH}(HDO)$ and $\nu_{OD}(HDO)$ bands. The lack of such resolution implies a much greater number of non-equivalent bonds, and hence implies a proton-disordered structure (there are 126 hydrogen bonds non-equivalent as to bonded-neighbor relationships in the disordered structure).

Discussion

The ice V structure represents a new type of tetrahedrally linked framework, which has no analog among known silica or tectosilicate structures. This is curious in view of the fact that the dense silica polymorph coesite has the same space group as ice V and has the same density relative to tridymite as has ice V relative to ice I, the tridymite-analog. In the coesite structure (Zoltai & Buerger, 1959) the main element is the 4-ring of linked tetrahedra, there being one 4-ring for every two silicon atoms. 4-rings are also present in ice V (ring O(2)-O(3'')-O(4')-O(4) in Fig. 1), but to the lesser extent of one 4-ring for every 3·5 H₂O molecules. The rings occur in pairs sharing an edge [O(4)-O(4')], and the pairs can be viewed as fragments of the coesite structure.

The lack of a silica-analog in the case of ice II could be explained (Kamb, 1964) on the basis of special structural features required by the proton ordering, which has no immediate counterpart in silica structures. No correspondingly definite explanation seems available for the unique tetrahedral framework of ice V. The structures of the denser forms ice VI and VII are not direct analogs of silica, but they are at least related in consisting of two interpenetrating frameworks of silica or tectosilicate type (Kamb & Davis, 1964; Kamb, 1965b). At high densities, packing requirements for oxygen in relation to tetrahedral linkage are certainly different for H₂O and SiO₂, and presumably this feature, as well as a difference in bond-bending flexibility in the two cases, is responsible for the distinction be-

tween the ice V and coesite-type frameworks. A particular instability for water frameworks with 4-ring linkages, abundant in the coesite type framework, does not seem indicated, because 4-rings do occur in ice V, they are abundant in ice VI (one 4-ring per 1·25 H₂O), and, though rare, they are known in clathrate hydrates (Beurskens & Jeffrey, 1964; Bode & Teufer, 1955).

Hydrogen bond lengths in tetrahedral groups around individual water molecules in ice V show a scatter comparable to that observed for Si-O distances in tectosilicates (Smith & Bailey, 1963), but, contrary to the silicates, there is no tendency for the average bond length within each individual tetrahedral group to be constant from one tetrahedral group to another. The bond lengths are correlated with ring connectivity in the framework: bonds not involved in 4-rings have lengths less than 2.79 Å, while bonds in 4-rings are longer than this, and the longest, 2.87 Å, is the bond common to two 4-rings.

The well-defined layers parallel to (001) in the structure, described earlier, are linked together only by bonds of type O(1)–O(3), and the approach of adjacent layers to one another is resisted directly by the short $O(3)\cdots O(4)$ distance of 3·28 Å (Fig. 1), and to a lesser extent by the $O(2)\cdots O(2)$ distance of 3·46 Å. Contrary to the case of ice II, however, where a similar situation involves a lengthening of the hydrogen bond to 2·84 Å, the O(1)–O(3) bond in ice V is only 2·78 Å. For geometrical reasons, the notable lengthening of the O(4)–O(4') bond to 2·87 Å cannot be attributed to repulsion at the short $O(3)\cdots O(4)$ contact. A simple interpretation of bond stretching in terms of the repulsion of close non-bonded neighbors cannot reliably be made for ice V (see Kamb, 1965b, p. 3923).

The areal density of hydrogen bonds linking adjacent (001) layers in ice V is 0.0573 Å^{-2} , scarcely larger than the density 0.0570 Å^{-2} of bonds between puckered hexagonal sheets parallel to (0001) in ice I. This suggests that for properties such as cleavage and plasticity, ice V should show anisotropy comparable to or greater than that shown by ice I (Nakaya, 1958).

The presence of proton disorder in ice V at temperatures within its stability field is indicated by its entropy (Kamb, 1964, p. 1446) and has been demonstrated by dielectric measurements (Wilson et al., 1965). The failure of ice V to undergo a transition to a protonordered structure at low temperature, as indicated by the structural and spectroscopic evidence for proton disorder in quenched ice V, is surprising in view of the considerable departure of the water molecule coordination from ideal tetrahedral (Table 5), which should energetically favor some water molecule orientations over others. From the measured dependence of dielectric relaxation time on temperature (Wilson, et al. 1965) it can be estimated that the dielectric relaxation time for ice V is about 1 sec at 170°K. This sets an upper limit on the temperature for transition to a possible ordered structure, hence the ordering energy (for disordering entropy 0.8 e.u.) must be less than 0.14 kcal.mole⁻¹. For comparison, the disordering energy for the ice II structure must be more than 0·24 kcal. mole⁻¹. Since an ordered structure for ice V in Aa is possible in which the average distortion of donor angles is no greater than in ice II (Table 5, angles marked with dagger), it seems necessary to conclude, as in the case of ice II (Kamb, 1964), that acceptor relationships play an important role in determining the hydrogen bond energies.

The crystallographic calculations were carried out with the CRYRM (IBM 7094) program written by R.E.Marsh, D.Duchamp, N.C.Webb, A.P.Kendig, C.M.Gramaccioli, T.A.Beineke, R.H.Stanford, and others. We are grateful to R.E.Marsh and R.Deverill for help with the computations. J.A.Doutt assisted in collecting the single-crystal data. The powder data at high pressure were obtained in collaboration with B.L. Davis.

References

Авганамя, S. C., Collin, R. L. & Lipscomb, W. N. (1951). Acta Cryst. 4, 15.

BARRETT, C. S. & MEYER, L. (1965). J. Chem. Phys. 43, 3502.

Bertie, J. E., Calvert, L. D. & Whalley, E. (1963). J. Chem. Phys. 38, 840.

Bertie, J. E. & Whalley, E. (1964). J. Chem. Phys. 40, 1646.

Beurskens, P. T. & Jeffrey, G. A. (1964). J. Chem. Phys. 40, 906.

BODE, H. & TEUFER, G. (1955). Acta Cryst. 8, 611.

Bridgman, P. W. (1912). Proc. Amer. Acad. Arts Sci. 47, 441.

BRIDGMAN, P. W. (1935). J. Chem. Phys. 3, 597.

BRIDGMAN, P. W. (1942). Proc. Amer. Acad. Arts Sci. 74, 399.

Busing, W. R. & Levy, H. A. (1965). J. Chem. Phys. 42, 3054.

CRAVEN, B. M., MARTINEZ-CARRERA, S. & JEFFREY, G. A. (1964). Acta Cryst. 17, 891.

CRAVEN, B. M. & TAKEI, W. J. (1964). Acta Cryst. 17, 415.

HIRSHFELDER, J. O., CURTISS, C. F. & BIRD, R. B. (1964). Molecular Theory of Gases and Liquids. New York: John Wiley.

HOERNI, J. A. & IBERS, J. A. (1954). Acta Cryst. 7, 744.

Honjo, G. & Shimaoka, K. (1957). Acta Cryst. 10, 710.

Howells, E. R., Phillips, D. C. & Rogers, D. (1950). *Acta Cryst.* 3, 210.

International Tables for X-ray Crystallography (1963). Vol. III. Birmingham: Kynoch Press.

JENSEN, L. H. & SUNDARALINGAM, M. (1964). Science, 145, 1185.

JORDAN, T. H., SMITH, H. W., STREIB, W. E. & LIPSCOMB, W. N. (1964). J. Chem Phys. 41, 756.

JORDAN, T. H., STREIB, W. E., SMITH, H. W. & LIPSCOMB, W. N. (1964). Acta Cryst. 17, 777.

JORDAN, T. H., STREIB, W. E. & LIPSCOMB, W. N. (1964). J. Chem. Phys. 41, 760.

KAMB, B. (1964). Acta Cryst. 17, 1437.

KAMB, B. (1965a). Science 150, 205.

KAMB, B. (1965b). J. Chem. Phys. 43, 3917.

KAMB, B. & DATTA, S. K. (1960). Nature, Lond. 187, 140; and unpublished work.

KAMB, B. & DAVIS, B. L. (1964). Proc. Nat. Acad. Sci. Wash. **52**, 1433.

Krüner, H. (1926). Z. Kristallogr. 63, 275.

NAKAYA, U. (1958). U.S. Snow, Ice, and Permafrost Res. Estab., Res. Report 82.

PAULING, L. (1935). J. Amer. Chem. Soc. 57, 2680. PAULING, L. (1960). The Nature of the Chemical Bond: Ithaca: Cornell Univ. Press.

Peterson, S. W. & Levy, H. (1957). Acta Cryst. 10, 70. PRAKASH, A. (1965). Z. Kristallogr. 122, 272.

ROLLETT, J. S. (1965). Computing Methods in Crystallography. Oxford: Pergamon Press.

SMITH, J. V. & BALIEY, S. W. (1963). Acta Cryst. 16, 801. VEGARD, L. (1930). Z. Phys. 61, 185.

WILSON, G. J., CHAN, R. K., DAVIDSON, D. W. & WHALLEY, E. (1965). J. Chem. Phys. 43, 2384.

ZOLTAI, T. & BUERGER, M. J. (1959), Z. Kristallogr. 111.

Acta Cryst. (1967). 22, 715

The Conformation of Non-Aromatic Ring Compounds.* XXXIV. The Crystal Structure of trans-2,3-Dichloro-1,4-thioxane at -185°C

By N. DE WOLF, C. ROMERS AND C. ALTONA Laboratory of Organic Chemistry, University of Leiden, The Netherlands

(Received 26 September 1966)

Crystals of trans-2,3-dichloro-1,4-thioxane are orthorhombic. The space group is $P2_12_12_1$, a=14.808, b=7.120, c=6.318 Å at -185 °C and Z=4. The structure has been solved by the heavy-atom technique and refined by use of eye-estimated Mo data (1813 observed reflexions) collected at -185°C, the final R value being 8.5%. The molecule has a chair conformation with the chlorine atoms in axial positions. Its overall geometry is halfway between the conformations of the corresponding trans-2,3-dichloro derivatives of 1,4-dioxane and 1,4-dithiane. A comparison is made with the corresponding halogenosubstituted dioxane, dithiane and 5- α -cholestane compounds.

Introduction

The conformational analysis of 1,4-thioxane and its halogeno-substituted derivatives forms a continuation of earlier investigations of the molecular shape of dioxane and dithiane compounds (cf. Table 5 for references). To our knowledge the conformations of 1,4thioxane and its halogeno derivatives have not yet been determined. From a study of electric dipole moments and nuclear magnetic resonance spectra of 1,4-thioxane and of trans-2,3-dichloro-1,4-thioxane (hereafter TDT) it is concluded (de Wolf, Henniger & Havinga, 1967) that these molecules are chair-shaped and that the chlorine atoms occupy axial positions. X-ray analysis of TDT corroborates these conclusions. The crystal structure of 1,4-thioxane will be dealt with in a separate paper.

Experimental

TDT is prepared by addition of chlorine to a solution of thioxene in carbon tetrachloride (Haubein, 1959). The crystals are brittle, colourless, irregular blocks which decompose in moist air. Two specimens, I and II, of cross-section 0.028×0.042 cm² and 0.02×0.02 cm² were sealed in Lindemann-glass capillaries and mounted on goniometer heads about the directions [001] and [010], respectively.

Glancing angles θ corresponding to spacings d(hk0)and d(h0l) were measured on zero layer Weissenberg photographs taken with copper radiation ($\lambda = 1.5418 \text{ Å}$) about [001] and [010] with crystals I and II, respectively. Aluminum powder lines (a=4.0489 Å at 20°C) were superposed on the films for calibration purposes. The unit-cell dimensions (Table 1) derived from these measurements were refined by a least-squares procedure and the stated errors are three times the calculated standard deviations in the cell edges. Absent reflexions h00 for h = odd, 0k0 for k = odd and 00l for l =odd determine the space group $P2_12_12_1$. The measured density (flotation method) indicates that the unit cell contains four molecules.

Intensity measurements (eye-estimation with a calibrated intensity strip) were recorded on equi-inclination Weissenberg photographs of the layers hk0

Table 1. Crystal data of TDT

trans-2,3-Dichloro-1,4-thioxane, C₄H₆OSCl₂. Melting point 37-38°C. Orthorhombic, P212121; $a = 14.808 \pm 0.012$, $b = 7.120 \pm 0.012$, $c = 6.318 \pm 0.015$ Å at -185 °C; $d_{\exp^{20}} = 1.64$, $d_x^{-185} = 1.73$ g.cm⁻³, Z = 4; F(000) = 352; $V = 666.1 \text{ Å}^3$; $\mu(Cu K\alpha) = 107 \text{ cm}^{-1}, \ \mu(Mo K\alpha) = 11.6 \text{ cm}^{-1}.$

^{*} Part XXXIII, C. Altona, H. R. Buys, H. J. Hageman & E. Havinga, to be published.